Cell Death and Differentiation (2001) 8, 631 – 639

www.nature.com/cdd

Pinocytic loading of cytochrome *c* into intact cells specifically induces caspase-dependent permeabilization of mitochondria: evidence for a cytochrome *c* feedback loop

KJ Gilmore[1], HE Quinn[1] and MR Wilson*[,1]

[1] Department of Biological Sciences, University of Wollongong, Northfields Avenue, Wollongong. NWS. 2522. Australia
* Author for correspondence: MR Wilson, Department of Biological Sciences, University of Wollongong, Northfields Avenue, Wollongong. NWS. 2522. Australia. Tel: 61-242-214534; Fax: 61-242-214135; E-mail: mrw@uow.edu.au

Received 9.10.00; revised 22.12.00; accepted 15.1.01
Edited by D Green

Abstract

Previous studies introduced cytochrome *c* into intact cells via the disruptive techniques of microinjection or electroporation to provide support for the hypothesis that, in whole cells, cytochrome *c* release from mitochondria triggers caspase activation and other degradative changes. However, the types of measurements that could be undertaken with these techniques was limited. We used the simple and relatively gentle technique of pinocytic loading to demonstrate that, in intact cells, cytosolic cytochrome *c* specifically induced activation of caspase-3- and -9-like enzymes, and a loss of mitochondrial polarization coincident with an increase in mitochondrial permeability. Our results support the prediction from *in vitro* studies that activation of caspases-3 and -9 is downstream of cytochrome *c* release and provide the first direct evidence that, in whole cells, cytochrome *c*-dependent caspase-activation can exert a feedback effect to elicit mitochondrial permeabilization and collapse of the mitochondrial trans-membrane potential. *Cell Death and Differentiation* (2001) **8,** 631 – 639.

Keywords: cytochrome *c*; caspase activation; mitochondrial permeabilization

Abbreviations: DFF, DNA fragmentation factor; BSA, bovine serum albumin; PT, permeability transition; DTT, dithiothreitol

Introduction

It is now generally accepted that, in many apoptotic systems, the release of pro-apoptotic proteins from mitochondria to the cytosol triggers the onset of degradative events such as DNA fragmentation.[1,2] The most extensively studied pro-apoptotic protein released from mitochondria is cytochrome *c*. The ability of cytochrome *c* to promote apoptotic changes was first reported by Liu *et al*,[4] who showed in a cell-free system that dATP and cytochrome *c* were both required to elicit caspase-3 activation and DNA fragmentation. Similar results were also reported for a different cell-free system based on *Xenopus* egg extracts.[4]

Subsequent work, again carried out using cell-free models of apoptosis, identified a series of molecular interactions that are initiated by the addition of dATP and cytochrome *c* (but not control proteins) to cytosol fractions, and that culminate in caspase activation and nuclear degradation. Thus, it is known that *in vitro*, cytochrome *c* forms a pro-apoptotic ternary complex with dATP, pro-caspase-9 and apoptotic protease activating factor 1 (Apaf-1) which leads to sequential activation of caspase-9, caspase-3, and DNA fragmentation factor (DFF).[5–7] Once activated, DFF initiates fragmentation of nuclear DNA.[7] Supporting the hypothesis that release of cytochrome *c* from mitochondria to the cytosol can trigger apoptotic degradation in intact cells, many studies have used cell fractionation techniques to demonstrate, for a wide variety of cell types, an apparent release of cytochrome *c* immediately prior to or coinciding with the onset of apoptotic changes (e.g.[8,9]). Similar findings have also come from studies using immunofluorescence with fixed, permeabilized cells[10] or selective permeabilization of cell membranes[11] to measure cytochrome *c* translocation.

More direct evidence that translocation of cytochrome *c* to the cytosol initiates apoptotic changes in intact cells was provided by reports that microinjection or electroporation of cytochrome *c* (but not control proteins) into cells elicits apoptotic changes such as cell shrinkage, nuclear condensation and exposure of the lipid phosphatidylserine on the cell surface.[12–14] These studies established, for a number of different intact cell types, that the pro-apoptotic effects of cytosolic cytochrome *c* are caspase-dependent and may specifically require caspase-3. However, for intact cells, no direct measurements of the effects of introduced cytosolic cytochrome *c* on the activation of different caspases have been made. Furthermore, although it has been repeatedly suggested that cytosolic caspases activated by cytochrome *c* release may act in a positive feedback loop to trigger changes in mitochondria resulting in further cytochrome *c* release and caspase activation,[15,16] only two studies have examined the effects of introduced cytosolic cytochrome *c* on mitochondria within intact cells. In one case, results from non-quantitative, direct fluorescence microscopic examination of cells stained with a fluorescent, potential-sensitive mitochondrial dye were interpreted as indicating that cytosolic cytochrome *c* had no effect on mitochondrial polarization.[14] In the second case, it was reported that loss of mitochondrial membrane potential ($\Delta\Psi_{mit}$) did not occur until immediately before cell death induced by microinjection of cytochrome *c*.[17] However, the validity of the technique used in this study

to measure changes in $\Delta\Psi_{mit}$ (staining cells with rhodamine 123) was questioned in recent reports.[18,19] Thus, it remains uncertain whether, in intact cells, the release of cytochrome *c* to the cytosol triggers quantitative changes in mitochondrial polarization or other mitochondrial changes.

We report that pinocytic loading, a mild non-invasive method for the introduction of macromolecules into intact cells,[20] is a suitable method for studying the effects of introducing cytochrome *c* into the cytosol of intact cells and demonstrate that this treatment specifically induced activation of caspase-3- and -9-like enzymes. Furthermore, we show that cytosolic cytochrome *c* specifically induced a caspase-dependent loss of mitochondrial membrane potential associated with an increase in mitochondrial permeability.

Results

Efficacy of pinocytic loading and pro-apoptotic effects of cytochrome *c* loading

Flow cytometric analysis of U937 and Jurkat cells pinocytically loaded with FITC-dextran indicated that most cells had taken up labelled macromolecule (Figure 1A). Dead cells were excluded from the analyses shown. However, even 3 h after pinocytic loading with hyper-osmotic buffer (with or without the addition of control proteins), the proportion of dead cells remained similar to that of untreated control cells, and comprised only 2–5% of the total population (data not shown). Thus, under the conditions used, the pinocytic loading treatment (including pinocytic loading of control proteins) had no significant effect on cell viability. Confocal analysis of cells showed that pinocytically loaded calcein was released to the cytosol (Figure 1B). Although similar results were obtained by confocal analysis of cells pinocytically loaded with FITC-dextran or FITC-cytochrome *c* (data not shown), the intensity of fluorescence obtained following pinocytic loading of calcein resulted in images of better quality.

Consistent with the results of earlier studies in which cytochrome *c* or control proteins were microinjected into live cells, we detected caspase-dependent apoptotic changes when cells were pinocytically loaded with (bovine) cytochrome *c* but not when they were loaded with control proteins. For example, pinocytic loading of cytochrome *c* (but not myoglobin) into Jurkat cells induced time-dependent internucleosomal fragmentation of DNA, which was inhibited by the broad spectrum caspase inhibitor zVADfmk (Figure 2A).

Furthermore, when stained with acridine orange, myoglobin-loaded cells showed large evenly-stained nuclei occupying most of the volume of the cytoplasm, while in many cytochrome *c*-loaded cells, nuclei showed an apoptotic morphology, appearing compacted and fragmented (Figure 2B). These changes were not detected when cells were pinocytically loaded from hyper-osmotic buffer containing other control proteins or no added protein (data

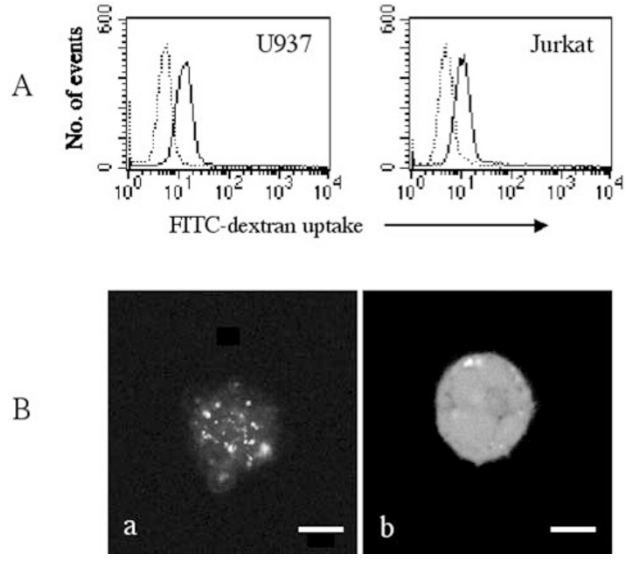

Figure 1 (**A**) Flow cytometry histogram overlays showing an increase in green fluorescence associated with U937 and Jurkat cells pinocytically loaded with 2×10^6Da FITC-dextran (solid lines) relative to untreated control cells (dotted lines). Dead cells were electronically excluded from the analyses. (**B**) Scanning confocal laser microscopy images showing U937 cells pinocytically loaded from a solution containing 2.3 mg/ml calcein. (a) During loading from hyper-osmotic buffer, calcein is found within pinocytic vesicles visible as localized regions of intense fluorescence. (b) Following exposure to hypo-osmotic buffer, calcein is released to the cytosol and is visible as fluorescence diffused throughout the bulk of the cell contents. Results shown are representative of several independent experiments. The horizontal white scale bars indicate 10 μm

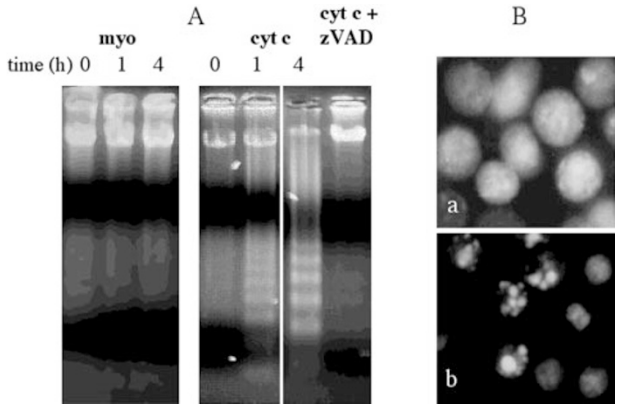

Figure 2 (**A**) Images of ethidium bromide-stained agarose gels showing specific induction of oligonucleosomal fragmentation of DNA resulting from pinocytic loading of cytochrome *c* into U937 cells. Cells were pinocytically loaded from hyper-osmotic buffer containing either 1 mg/ml myoglobin (myo) or 1 mg/ml cytochrome *c* (cyt *c*) and then incubated for various periods of time at 37°C before DNA was purified from the cells and analyzed by agarose gel electrophoresis. The appearance of 'DNA ladders' in the lanes corresponding to cytochrome *c*-loaded cells (at 1 and 4 h) indicated that cytochrome *c* specifically induced internucleosomal fragmentation of DNA. The far right lane represents DNA that was purified from cells that had been co-loaded from hyper-osmotic buffer containing 1 mg/ml cytochrome *c* and 50 μM zVADfmk and incubated for 4 h at 37°C. The dark horizontal bands on the images are the result of fluorescence quenching by the tracker dyes. Similar results were obtained when Jurkat cells were pinocytic loaded with cytochrome *c* (data not shown). (**B**) Fluorescence micrographs showing Jurkat cells stained with acridine orange 2 h after pinocytic loading with myoglobin (a) or cytochrome *c* (b)

not shown). Other cytochrome *c*-specific effects included cell shrinkage and externalization of phosphatidylserine (data not shown). Pinocytic loading of cytochrome *c* purified from horse heart produced similar specific pro-apoptotic effects (data not shown).

Pinocytic loading of cytochrome *c* induces specific activation of caspase-3- and -9-like enzymes

Earlier studies have shown that, under appropriate conditions, the addition of cytochrome *c* to cytosol fractions prepared from cells induces activation of caspase-3 and -9. However, it was not previously possible to measure whether the introduction of cytochrome *c* into intact cells specifically induced an increase in the activity of these caspases. Lysates were prepared from cells at intervals following pinocytic loading of cytochrome *c* or control proteins and tested in fluorometric microplate assays for specific caspase activities (see Materials and Methods). Pinocytic loading of cytochrome *c* induced much higher levels of activation of caspase-3 and -9-like enzymes that did pinocytic loading of control proteins (e.g. myoblobin, BSA) or hyper-osmotic buffer alone (i.e. without any added protein) (Figure 3). For both cell types, caspase activation was detected in lysates prepared from cells 10 min after pinocytic loading of cytochrome *c*. Caspase-3- and -9-like activities peaked at 1 – 2 h following loading and appeared to decline thereafter (most rapidly for caspase-3-like activity in U937 cells). When allowance is made for the different number of each cell type used in each assay (see Materials and Methods), on a per cell basis, the maximum level of activation of caspase-3-like enzymes was about twofold greater in U937 cells than in Jurkat cells. On the same basis, the maximum level of activation of caspase-9-like enzymes was similar in both U937 and Jurkat cells.

In U937 cells, cytochrome *c* loading appeared to induce a higher level of activation of caspase-3-like enzymes *versus* caspase-9-like enzymes (Figure 3, a *vs* c). A similar trend was found for cytochrome *c* loading of Jurkat cells, although in this case the difference was less. However, it is difficult to draw quantitative conclusions from this data because the differences may be explained in part by differences in the affinities of the enzymes for their respective substrates. In proportion to cytochrome *c*-specific induction of caspase activation, the pinocytic loading treatment appeared to induce in U937 cells a higher level of non-specific activation of caspase-9-like enzymes than was the case for caspase-3-like enzymes (Figure 3, c *vs* a). The reason for this difference is not clear, however, it is known that the specificity of the peptide-based caspase substrates/inhibitors is not abso-

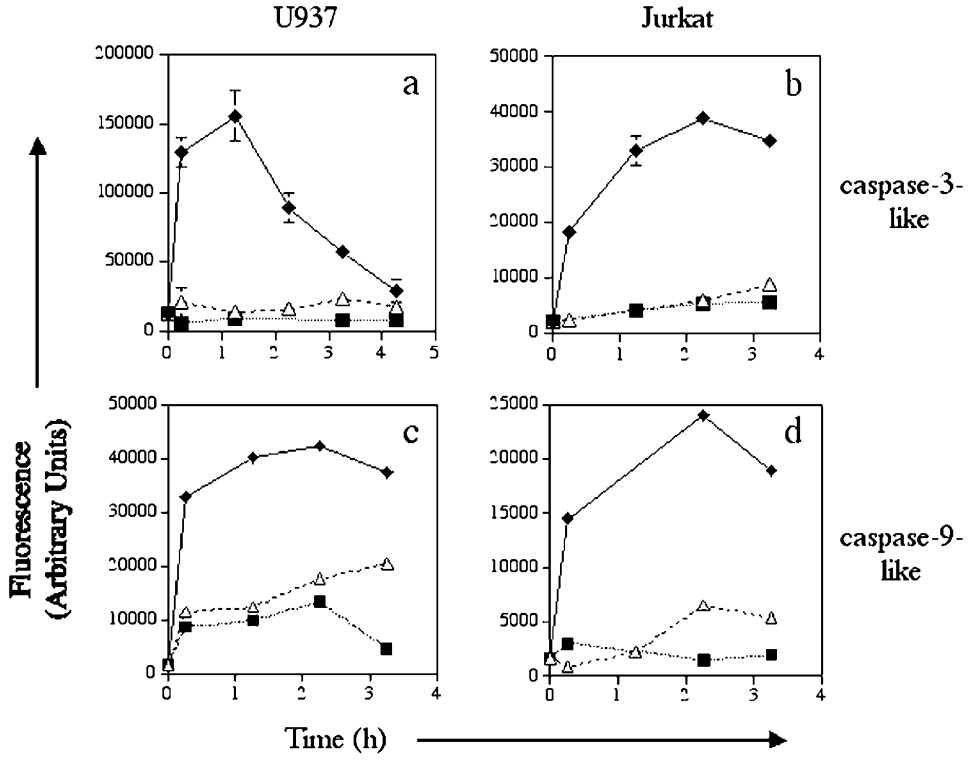

Figure 3 Activities of caspase-3- and -9-like enzymes in cell lysates, as a function of time following pinocytic loading from solutions containing either no added protein (△), 1 mg/ml myoglobin (■), or 1 mg/ml cytochrome *c* (◆). For measurements of caspase-3-like activity, 12 μg of cell lysate protein was added to each assay well. For measurements of caspase-9-like activity, this amount was increased to 24 μg per well. Activities are expressed as arbitrary units of AMC fluorescence (see Materials and Methods for details of assay). Data points represent means of triplicate measurements and, in each case, the error bars shown are standard errors (S.E.) of the mean. In many cases, the S.E. are too small to be visible. When the caspase inhibitors DEVD.CHO or LEHD.CHO were added to wells containing cell lysate and, respectively, DEVD.AMC or LEHD.AMC, negligible levels of fluorescence were detected (data not shown). The results shown are representative of several independent experiments

lute.[21] Furthermore, it is relevant to note that zVADfmk was recently shown to inhibit the non-caspase protease calpain.[22] Thus, it is possible that, when prepared as described, U937 cell lysates contained non-caspase enzyme(s) capable of cleaving the LEHD-AMC substrate. An alternative explanation is that for unknown reasons, the pinocytic loading treatment induced in U937 cells a significant level of activation of caspase-9-like enzymes, albeit at a lower level to that induced by cytosolic cytochrome *c*.

In other similar experiments we found that pinocytic loading of cytochrome *c* induced activation of caspase-8-like enzymes to a level that was only slightly above that detected for control cells (data not shown). Thus, pinocytic loading of cytochrome *c* specifically activated caspase-3- and -9-like enzymes but had less effect on caspase-8-like enzymes. Since the peptide substrates used in the microplate caspase assays are not absolutely specific,[21] we analyzed cell lysates by immunoblotting to confirm that pinocytic loading of cytochrome *c* specifically activated caspase-3 and caspase-9. This was found to be the case (data not shown).

The broad spectrum caspase inhibitor zVAD.fmk and the caspase-3-like enzyme inhibitor DEVD.CHO both virtually abolished activation of caspase-3-like enzymes induced by pinocytic loading of cytochrome *c* (Figure 4A). Under the same conditions, the caspase-9 inhibitor LEHD.CHO inhibited activation of caspase-9-like enzymes in U937 and Jurkat cells (data not shown). Furthermore, co-loading LEHD.CHO with cytochrome *c* potently inhibited activation of caspase-3-like enzymes in U937 cells and gave similar but lesser inhibition in Jurkat cells (Figure 4B).

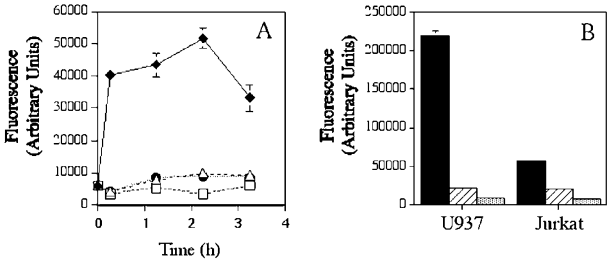

Figure 4 (**A**) Activity of caspase-3-like enzymes in Jurkat cell lysates, as a function of time following pinocytic loading from solutions containing either no added protein (△), 1 mg/ml cytochrome *c* (◆), or 1 mg/ml cytochrome *c* together with either 50 μM zVADfmk (●) or 100 μM DEVD.CHO (□). Activities are expressed as arbitrary units of AMC fluorescence. Data points represent means of triplicate measurements and, in each case, the error bars shown are standard errors (S.E.) of the mean. In many cases, the S.E. are too small to be visible. When the caspase inhibitor DEVD.CHO was added to wells containing cell lysate and DEVD.AMC, negligible levels of fluorescence were detected (data not shown). Similar results were obtained with U937 cells (data not shown). (**B**) Bar graph showing the level of caspase-3-like activity in lysates prepared from U937 and Jurkat cells 2 h after pinocytic loading with cytochrome *c*. Cells were loaded from hyper-osmotic buffer containing 1 mg/ml cytochrome *c* either with (striped bars) or without (solid bars) the addition of 500 μM LEHD.CHO. The shaded bars indicate the corresponding activities in lysates prepared from cells pinocytically loaded from hyper-osmotic buffer containing no added protein. Activities are expressed as arbitrary units of AMC fluorescence. Data points represent means of triplicate measurements and, in each case, the error bars shown are standard errors (S.E.) of the mean. In most cases, the S.E. are too small to be visible

Pinocytic loading of cytochrome *c* induces caspase-dependent mitochondrial depolarization and an increase in mitochondrial permeability

Pinocytic loading of cytochrome *c* specifically induced mitochondrial depolarization in both U937 and Jurkat cells, the effect increasing with time and generally reaching a maximum at 2–3 h after loading (Figure 5). In other independent experiments, cytochrome *c* loading induced mitochondrial depolarization in 30–50% of cells (data not shown). Variations between experiments in the level of response may be due to differences in the efficiency of pinocytic loading. The extent to which molecules are pinocytically loaded into individual cells is not constant but varies across a defined range (see Figure 1A). The fact that not all cells showed loss of mitochondrial membrane potential may indicate that only those cells with the highest levels of cytochrome *c* uptake underwent this change. Even in those cells with the highest level of uptake, the amount of cytochrome *c* introduced into the cytosol is probably significantly less than that available from endogenous stores (see Discussion)

For both cell types tested, co-loading of zVAD.fmk or DEVD.CHO strongly inhibited cytochrome *c*-induced mitochondrial depolarization (Figure 5). These results indicate that cytochrome *c*-induced mitochondrial depolarization is caspase-dependent and is downstream of the activation of caspase-3-like enzymes. Confocal microscopic examination of cells simultaneously stained with FITC-VAD and CMXRos, after pinocytic loading with cytochrome *c*, revealed a clear inverse relationship between caspase activation and mitochondrial polarization (Figure 6). Cells containing activated caspases were cytoplasmically labelled with green fluorescence and had reduced or absent mitochondrial red fluorescence. Conversely, cells that lacked activated caspases lacked cytoplasmic green fluorescence and had visibly stronger red fluorescence

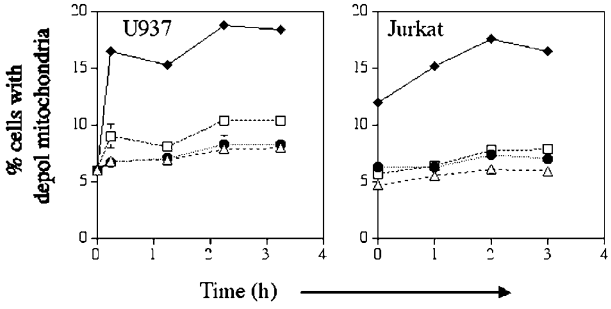

Figure 5 Line graphs showing the proportion of U937 and Jurkat cells with reduced mitochondria membrane potential following pinocytic loading from hyper-osmotic buffer containing either no added protein (△), 1 mg/ml cytochrome *c* (◆), or 1 mg/ml cytochrome *c* and either 50 μM zVADfmk (●) or 100 μM DEVD.CHO (□). Data points are means of triplicate determinations and, in each case, the error bars shown are standard errors (S.E.) of the mean. In many cases, the S.E. are too small to be visible. Like cells loaded from hyper-osmotic buffer lacking any added protein, the fraction of cells pinocytic loaded with control proteins (e.g. myoglobin, BSA) found to have depolarized mitochondria was similar to that measured for untreated control cells (data not shown)

associated with their mitochondria (Figure 6). Taken together, these results indicate that in intact U937 and Jurkat cells, cytochrome *c*-induced activation of caspases induces collapse of $\Delta\Psi_{mit}$ downstream of the activation of caspase-3-like enzymes.

Confocal microscopic analysis of pinocytically-loaded cells confirmed that cytochrome *c* induced loss of $\Delta\Psi_{mit}$ coincided with an increase in mitochondrial permeability (Figure 7). Following pinocytic loading with hyper-osmotic buffer containing calcein and either no other additions or control proteins, most cells showed an uneven distribution of calcein in the cytoplasm. Calcein was excluded from a number of regions in the cytoplasm, which appeared as dark areas in a background of green fluorescence (Figure 7a). Staining of these cells with TMRM indicated that many of the regions excluding calcein corresponded to polarized mitochondria, detected as regions of bright red fluorescence (Figure 7b and c). In contrast, after pinocytic co-loading of calcein and cytochrome *c* (but not following co-loading of calcein and other control proteins), many cells showed a more even distribution of calcein fluorescence throughout the cytoplasm, with a reduction in the number and intensity of dark (non-fluorescent) regions detected (Figure 7d). This difference coincided with a marked reduction in the level of red TMRM fluorescence associated with mitochondria (Figure 7e and f). The cytochrome *c*-induced changed were inhibited by co-loading cells with either zVADfmk or DEVD.CHO (data not shown). Taken together with results described above, these results indicate that in U937 and Jurkat cells, cytosolic cytochrome *c* specifically induced caspase-dependent mitochondrial permeabilization and an associated collapse of $\Delta\Psi_{mit}$.

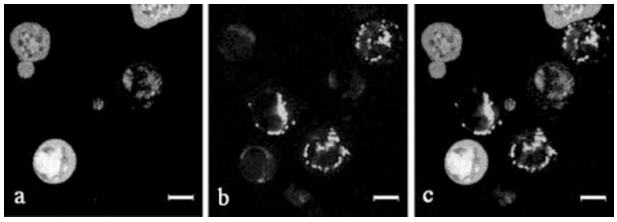

Figure 6 Confocal microscopic images of Jurkat cells simultaneously stained with FITC-VAD (green fluorescence indicating caspase activation) and CMXRos (red fluorescence indicating polarized mitochondria) 1 h after pinocytic loading with cytochrome *c*. Panels represent FITC-VAD fluorescence only (**a**), CMXRos fluorescence only (**b**), and an overlay of the two previous images (**c**). Images shown are representative of many acquired. Similar results were obtained with U937 cells (data not shown). The horizontal white scale bars indicate 10 μm

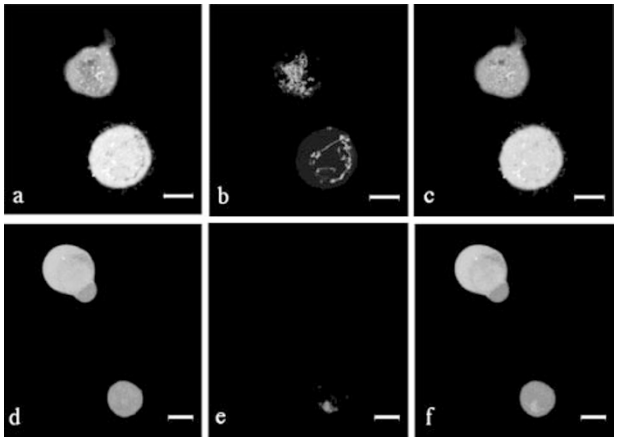

Figure 7 Confocal microscopic images of Jurkat cells demonstrating that pinocytic loading of cytochrome *c* induces mitochondrial permeabilization. Cells were pinocytically loaded from hyper-osmotic buffer containing 2.3 mg/ml calcein either without (**a–c**) or with (**d–f**) the addition of 1 mg/ml cytochrome *c*. The intracellular distribution of calcein is indicated by green fluorescence (**a** and **d**). Cells were counterstained with TMRM to indicate mitochondrial polarization (red fluorescence; **b** and **e**). Panels **c** and **f** show overlays of the two preceding images, respectively. The horizontal white scale bars indicate 10 μm. The images shown are representative of several independent experiments. Similar results were obtained with U937 cells (data not shown). Superior images were obtained with Jurkat cells due to their larger size and the fact that U937 cells rapidly fragment to form apoptotic bodies after cytochrome *c* loading. Results similar to those shown in **a–c** were obtained when cells were pinocytically loaded with control proteins (e.g. myoglobin, BSA), or when cytochrome *c* was co-loaded with either of the caspase inhibitors zVADfmk or DEVD.CHO (data not shown)

Discussion

Most previous investigations of the ability of cytochrome *c* to elicit apoptotic changes in intact cells introduced the protein into cells via microinjection.[12,13,17,23–26] This imposed severe practical constraints, limiting the numbers of cells that could be analyzed to the order of hundreds or less and restricting most measurements to observations of morphological changes, such as cell shrinkage, membrane blebbing and nuclear compaction. In agreement with these earlier studies, we found that pinocytic loading of cytochrome *c* (but not control proteins) induced the same range of morphological changes typical of apoptosis. Furthermore, we were able to exploit the ability of pinocytic loading to introduce proteins into large numbers of cells to demonstrate that loading of cytochrome *c* into U937 and Jurkat cells specifically induced internucleosomal DNA fragmentation (detected by agarose gel electrophoresis) and externalization of phosphatidylserine (detected by flow cytometric analysis; data not shown).

An earlier report used electroporation to study the pro-apoptotic effects of introducing cytochrome *c* into intact cells.[14] Although electroporation is a viable technique to introduce macromolecules into live cells, its efficiency is often low and the treatment is relatively harsh, resulting in losses in cell viability that may compromise subsequent analyses. This was reflected in the observations that: (i) labelled cytochrome *c* was taken up by only 24% of electroporated Bo cells; (ii) between 20 and 50% of control cells lysed within 1 h of electroporation; and (iii) in the surviving cells apoptosis ranged from undetectable to nearly 20%.[14] Preliminary experiments with U937 and HL60 cells indicated even higher levels of electroporation-induced apoptosis (data not shown). For the cell types tested, we found that pinocytic loading was a far gentler method for introducing macromolecules into cells. Pinocytic loading very efficiently introduced labelled macromolecules into both U937 and Jurkat cells with limited effects on cell viability. In

preliminary experiments, pinocytic loading, even in the absence of any added proteins, was found to negatively affect the viability of HL60 cells (data not shown), indicating that some cell types are more sensitive to the treatment than others. Nevertheless, pinocytic loading appears to be a technique generally well suited to studying the effects of introducing cytochrome *c* into whole cells.

By loading cells with FITC-labelled cytochrome *c*, and measuring the fluorescence of cell lysates relative to FITC-cytochrome *c* standards, we estimated that the pinocytic loading protocol described delivered about 12 fg of cytochrome *c* into each Jurkat cell and about 16 fg of cytochrome *c* into each U937 cell (data not shown). The total mitochondrial content of cytochrome *c* in kidney 293 and MCF-7 cells was estimated as 40–100 fg/cell.[12] Since Jurkat and U937 cells are likely to have a similar mitochondrial cytochrome *c* content, the amounts introduced into individual cells by pinocytic loading probably correspond to significantly less than could be released from endogenous mitochondrial stores. Therefore, the amounts of cytochrome *c* delivered into cells in this study were physiologically relevant.

We demonstrated by fluorometric assay that pinocytic loading of cytochrome *c* into the cytosol of intact cells specifically induced activation of caspase-3- and -9-like enzymes. Furthermore, we confirmed by immunoblotting that pinocytic loading of cytochrome *c* induced proteolytic activation of caspase-3 and caspase-9 (data not shown). The results of studies of cell-free systems[3,6] have suggested that the release of cytochrome *c* from mitochondria to the cytosol triggers the formation of a tetramolecular complex between cytochrome *c*, dATP, Apaf-1 and pro-caspase-9 (the 'apoptosome'[1]), leading to sequential activation of caspase-9, caspase-3 and thence DNA fragmentation. Our results confirm that in whole cells, cytosolic cytochrome *c* triggers activation of caspase-9-like and caspase-3-like enzymes and leads to internucleosomal DNA fragmentation.

Our demonstration that, when co-loaded with cytochrome *c*, the caspase-9 inhibitor LEHD.CHO inhibited activation of both caspase-9- and -3-like enzymes is consistent with the proposed sequence of events deduced from studies of cell-free systems, in which active caspase-9 is responsible for proteolytic activation of caspase-3.[1] However, the specificity of peptide inhibitors like LEHD.CHO is not absolute.[21] Therefore, the possibility that LEHD.CHO may have directly inhibited caspase-3-like enzymes under the conditions tested cannot be excluded.

It was recently demonstrated in a cell-free system that the addition of cytochrome *c* to Jurkat cell extract containing mitochondria resulted in the release of cytochrome *c* from the mitochondria coincident with caspase-3 activation.[27] These results support the hypothesis that, in intact cells, cytochrome *c* release might exert a feedback effect on mitochondria (via caspase activation) to amplify further cytochrome *c* release. Our results provide the first direct evidence obtained working with intact cells that mitochondrial release of cytochrome *c* to the cytosol does initiate a feedback effect on mitochondria. We demonstrated that pinocytic loading of cytochrome *c* into intact cells specifically induced mitochondrial depolarization which was associated with an increase in mitochondrial permeability. The cytochrome *c*-induced loss of $\Delta\Psi_{mit}$ was detected in many independent experiments utilizing three different widely used mitochondrial potential sensitive dyes ($DiOC_6$, CMXRos and TMRM).[19,28,29] The effects of cytosolic cytochrome *c* on mitochondria were potently inhibited by zVADfmk and DEVD.CHO, suggesting that activation of caspase-3-like enzymes was directly or indirectly responsible for the mitochondrial changes measured.

The entry of cytosolic calcein into mitochondria we detected is consistent with a mitochondrial permeability transition, which has been shown *in vitro* to cause the release of endogenous mitochondria cytochrome *c*.[30,31] However, the current data do not allow us to exclude the possibility that calcein entered only the intermembrane space (including the lumen of the cristae) and that mitochondrial depolarization resulted from a loss of integrity of the outer mitochondrial membrane. In either case, our results are consistent with the suggestion that cytosolic caspases activated by cytochrome *c* release act on mitochondria to cause further cytochrome *c* release and caspase activation.[15,16,32] It is uncertain whether, in intact cells, caspases can directly elicit pro-apoptotic changes in mitochondria or whether they exert these effects exclusively by proteolytic activation of other molecules (e.g. Bid[33,34]). The former possibility is supported by *in vitro* demonstrations that recombinant caspases act on isolated mitochondria to induce permeability transition and cytochrome *c* release.[32,35] The latter possibility is supported by the recent demonstration in a cell-free system that cytochrome *c* triggers caspase-3-dependent activation of Bid, which is known to translocate to mitochondria to induce cytochrome *c* release.[27] Therefore, the available evidence is consistent with the hypothesis that, *in vivo*, caspases may elicit pro-apoptotic mitochondrial changes via more than one pathway.

To summarize, we have shown that pinocytic loading is a suitable technique to study the specific effects of introducing cytochrome *c* into large numbers of intact cells. Working with whole cell systems, pinocytic loading offers an alternative to transfection, microinjection or electroporation for studies of proteins thought to regulate apoptosis. The technique is simple and inexpensive, does not require any specialized equipment, and in suitable cell types produces only low level non-specific effects. We used this approach to demonstrate that the introduction of cytochrome *c* into the cytosol of intact cells specifically triggered activation of caspase-3- and -9-like enzymes and loss of $\Delta\Psi_{mit}$ associated with an increase in mitochondrial permeability. Importantly, our results demonstrate that, in intact cells, at a point downstream of the activation of caspase-3-like enzymes, cytochrome *c*-induced caspase activation exerts a feedback effect on mitochondria which would be expected to release more cytochrome *c* and amplify the apoptotic cascade. The proposed cytochrome *c* feedback mechanism may play an important role in cell death pathways in which initial cytochrome *c* release occurs independently of caspase activation.

Materials and Methods

Reagents

DMEM : F12 and foetal bovine serum (FBS) were purchased from Trace Biosciences (Melbourne, Australia) and sterile plasticware was obtained from Interpath Services (Melbourne, Australia). Acridine orange, acrylamide, agarose, casein, (3-[(3-cholamidopropyl)-dimethylamonio]-1-propanesulfonate) (CHAPS), cytochrome *c* (from bovine heart), ethylenediamine tetraacetic acid (EDTA), ethylene glycol-bis(β-aminoethylether)-N,N,N′,N′-tetraacetic acid (EGTA), fluorescein isothiocyanate-labelled dextran (FITC-dextran, molecular mass 2×10^6 Da), N,N′-methylenebis-acrylamide, myoglobin (from horse heart), piperazine-N,N′-bis-[2-ethanesulphonic acid] (PIPES), polyethlene glycol (molecular mass 1000 Da; PEG1000), propidium iodide (PI) and sucrose were obtained from Sigma (Sydney, Australia). FITC-cytochrome *c* was produced by coupling FITC to bovine cytochrome *c* using standard methods. N-(2-hydroxyethyl)piperazine-N′-(2-ethanesulphonic acid) (HEPES) was purchased from United States Biochemical Corp. (OH, USA). The caspase inhibitors DEVD.CHO and LEHD.CHO and caspase substrates DEVD.AMC and LEHD.AMC were obtained from BIOMOL (PA, USA). The caspase inhibitor zVAD.fmk was purchased from Calbiochem (Sydney, Australia). FITC-VADfmk was purchased from Promega (Sydney, Australia). Costar black fluoro-assay microtitre plates were obtained from Corning (MA, USA). Complete® protease inhibitor cocktail and dithiothreitol (DTT) were purchased from Boehringer Mannheim (Sydney, Australia). 3,3′-Dihexyloxacarbocyanine iodide ($DiOC_6$), chloromethyl-X-rosamine (CMXRos), calcein and tetramethylrhodamine methyl ester (TMRM) were purchased from Molecular Probes Inc. (OR, USA). All other chemicals were of analytical reagent grade and were purchased from Ajax Chemicals (Sydney, Australia) or BDH Chemicals (Dorset, UK).

Cell culture

The human leukaemic cell lines Jurkat (T-cell) and U-937 (myelomonocytic) were obtained from the American Type Culture Collection (ATCC, MD, USA). Cells were cultured in complete medium (DMEM : HAMS F12 supplemented with 10% (v/v) FBS) at 37°C in a humidified atmosphere of 5% CO_2.

Pinocytic loading

Pinocytic loading of macromolecules into cells was performed similarly to the method described in Okada and Rechsteiner.[20] Culture containing $2-10 \times 10^6$ cells was centrifuged (500 *g*, 5 min) and the cells resuspended in 200 μl of hyper-osmotic buffer (10 mM HEPES, pH 7.4, 10% (w/v) PEG1000, 0.5 M sucrose) containing either no additions, 2.3 mg/ml calcein, 1 mg/ml of FITC-dextran or FITC-cytochrome *c*, or 1 mg/ml of cytochrome *c*, myoglobin or other control proteins (e.g. bovine serum albumin). After a 10 min incubation at 37°C, the cell suspension was diluted to 10 ml with hypo-osmotic buffer (60% DMEM : F12: 40% water (v/v)) and incubated for 2 min at 37°C. The cells were then centrifuged (500 *g*, 5 min) and resuspended at 1×10^6 cells/ml in complete medium. In later experiments it was found that the hypo-osmotic wash step was unnecessary and cells were washed instead in undiluted DMEM : F12. Uptake of FITC-dextran was measured by flow cytometric analysis, performed using a FACSort flow cytometer (Becton Dickinson, Sydney, Australia). For each analysis, 10 000 cells were acquired, collecting signals for forward and side angle laser scatter and green (FL1) and red (FL3) fluorescence. Immediately prior to analysis, 1 μg/ml of propidium iodide (which stains dead cell nuclei brightly fluorescent) was added to each cell suspension. Dead cells were electronically excluded from the analyses. Data was acquired and analyzed using CellQuest software (v3.1f; Becton Dickinson, Sydney, Australia). Transfer of pinocytically loaded calcein to the cytosol was confirmed by scanning laser confocal microscopy using a Leica DMIRBE inverted microscope coupled to a Leica TCS SP confocal system (Leica Microsystems, Sydney, Australia). Cells were excited at 488 nm and fluorescence collected using an emission window set at 500–540 nm. To test the effects of caspase inhibition, in some experiments, cells were pinocytically loaded as above from solutions containing cytochrome *c* and either 50 μM zVAD.fmk, 100 μM DEVD.CHO or 500 μM LEHD.CHO.

Analysis of DNA fragmentation and changes in nuclear morphology

In some experiments, at intervals following pinocytic loading with cytochrome *c* or control proteins, 2×10^6 cells were washed with phosphate buffered saline (PBS) and then either stained for 5 min with 4 μM acridine orange or frozen at -20°C for subsequent extraction of DNA. Acridine orange-stained cells were washed twice with PBS before being examined by fluorescence microscopy. DNA was purified from frozen cells using standard methods (proteinase K/SDS lysis followed by phenol : chloroform extractions) and then analyzed by electrophoresis on 1% agarose gels.

Fluorescence-based caspase activation assays

Caspase-3- and -9-like activities were measured using a fluorometric microplate assay adapted from Enari *et al*.[36] Activity was measured as fluorescence following the addition of an appropriate fluorogenic peptide substrate (aminomethylcoumarin (AMC) derivative) to cell lysates. Measurements were made of the fluorescence produced in the presence and absence of a specific tetrapeptide aldehyde inhibitor; the difference indicated the level of caspase-mediated substrate cleavage. The substrate and inhibitor pair used to measure caspase-3-like activity were, respectively, DEVD.AMC and DEVD.CHO. The corresponding substrate and inhibitor pair used to measure caspase-9-like activity were, respectively, LEHD.AMC and LEHD.CHO.

For assay of caspase-3-like enzymes, for each sample, 2×10^6 U937 cells or 1×10^6 Jurkat cells were centrifuged (500 *g*, 5 min) and frozen at -80°C until required. For assay of caspase-9-like enzymes, the procedure was the same except 4×10^6 U937 or 2×10^6 Jurkat cells were used. Cells were lysed by repeated freeze-thawing in 150 μl of extraction buffer (50 mM PIPES-NaOH, pH 7.0, 50 mM KCl, 5 mM EGTA, 2 mM $MgCl_2$, 1 mM DTT, Complete® protease inhibitor cocktail) and then centrifuged at 8000 *g* for 15 min at 4°C. For all assays of caspase-3-like enzymes, regardless of cell type, the supernatant contained about 120 μg of protein. Similarly, for assays of caspase-9-like enzymes, regardless of cell type, the supernatant contained about 240 μg of protein. In each case, the supernatant was diluted with 350 μl of assay buffer (100 mM HEPES-KOH, pH 7.5, 10% (w/v) sucrose, 0.1% (w/v) CHAPS, 10 mM DTT, 0.1 mg/ml ovalbumin) and 50 μl aliquots dispensed into each of three wells of a black fluoro-assay microtitre plate. The appropriate caspase inhibitor (diluted in assay buffer) was added to the triplicate wells to a final concentration of 1 μM (DEVD.CHO) or 10 μM (LEHD.CHO) and pre-incubated at 37°C for 30 min. Following the 30 min incubation, 50 μl aliquots of lysate (previously held on ice) were added to six additional wells on the microplate. To the triplicate wells containing the inhibitor and a further three wells, the appropriate caspase substrate was

added to a final concentration of 10 μM (DEVD.AMC) or 20 μM (LEHD.AMC). Assay buffer only was added to the remaining three (background) wells and the plates were incubated for 1–2 h at 37°C. Contents of wells were excited at 390 nm and the fluorescence emitted at 460 nm measured using a Biolumin 960 fluorescence plate reader operated by Xperiment software (v.1.1.0) (Molecular Dynamics; CA, USA). As the specificity of the fluorogenic substrates and inhibitors is not absolute,[21] cleavage of a fluorogenic substrate was interpreted as indicating activation of the target caspase or of a closely related caspase.

General activation of caspases was measured using FITC-VADfmk (FITC-VAD), following the manufacturer's instructions. FITC-VAD is a fluorescent, cell-permeable inhibitor that binds irreversibly to activated caspases. By incubating cells with 10 μM FITC-VAD for 20 min and subsequently washing them, cells containing activated caspases become cytoplasmically labelled with green fluorescence. Labelling of cells with FITC-VAD was detected by confocal microscope analysis, performed as described above.

Flow cytometric analyses of mitochondrial membrane potential

Changes in mitochondrial membrane potential ($\Delta\Psi_{mit}$) were measured using the cationic lipophilic fluor $DiOC_6$ which accumulates to an extent dependent upon $\Delta\Psi_{mit}$ in the negatively charged mitochondrial matrix.[37] For each test, 5×10^5 cells were suspended in 0.5 ml of complete medium containing 40 nM $DiOC_6$ and incubated in the dark for 15 min at 37°C. In all cases, 1 μg/ml of propidium iodide was added to each cell suspension immediately before flow cytometric analysis which was performed as described above. Using CellQuest software (v3.1f; Becton Dickinson, Sydney, Australia), fluorescence histograms were first drawn for control cells and the proportion of treated cells with green fluorescence less than that of the controls calculated using the statistics functions of the software. Dead cells were electronically excluded from the analyses.

Confocal microscopic analyses of changes in caspase activation, mitochondrial membrane potential and mitochondrial permeability

For concurrent analysis of caspase activation and changes in $\Delta\Psi_{mit}$, 2×10^6 cells (that had previously been pinocytically loaded with cytochrome *c* or control proteins and incubated at 37°C for 1 h) were incubated (protected from light) for 20 min at 37°C in complete medium containing 10 μM FITC-VAD and 100 nM CMXRos. Cells were then washed twice in complete medium containing 100 nM CMXRos before being immediately examined by confocal microscopy. Cells were sequentially excited at 488 nm (FITC-VAD) and 543 nm (CMXRos) and fluorescence collected using emission windows set at 500–535 nm (FITC-VAD) and 580–640 nm (CMXRos).

Confocal microscopy has been used to measure mitochondrial permeability transition (PT) in intact cells by following the movement of calcein (a 622 Da fluor) into or out from mitochondria (resulting from opening of the PT megapores).[38,39] We used a similar approach to better define the effects of cytosolic cytochrome *c* on mitochondria within intact cells. Calcein was introduced into the cytosol by pinocytic loading, as described above, from an external concentration of 2.3 mg/ml. In some cases, cells were simultaneously loaded with calcein and cytochrome *c* (or control proteins). For concurrent measurement of $\Delta\Psi_{mit}$, following pinocytic loading, 2×10^6 cells were incubated (protected from light) for 15 min at 37°C in 500 μl of complete medium containing 100 nM TMRM. The cells were then immediately examined by confocal microscopy. Cells were sequentially excited at 488 nm (calcein) and 543 nm (TMRM) and fluorescence collected using emission windows set at 500–540 nm (calcein) and 560–610 nm (TMRM).

Acknowledgements

We thank Simon Easterbrook-Smith and Ulf Brunk for critical review of the manuscript.

References

1. Green DR and Reed JC (1998) Mitochondria and apoptosis. Science 281: 1309–1312
2. Wilson MR (1998) Apoptosis: unmasking the executioner. Cell Death Differ. 5: 646–652
3. Liu XS, Kim CN, Yang J, Jemmerson R and Wang XD (1996) Induction of apoptotic program in cell-free extracts – requirement for dATP and cytochrome c. Cell 86: 147–157
4. Kluck RM, Bossywetzel E, Green DR and Newmeyer DD (1997) The release of cytochrome c from mitochondria – a primary site for Bcl-2 regulation of apoptosis. Science 275: 1132–1136
5. Zou H, Henzel WJ, Liu XS, Lutschg A and Wang XD (1997) Apaf-1, a human protein homologous to C. Elegans Ced-4, participates in cytochrome c-dependent activation of caspase-3. Cell 90: 405–413
6. Li P, Deepak Nijhawan, Budihardjo I, Srinivasula SM, Ahmad M, Alnemri ES and Wang X (1997) Cytochrome c and dATP-dependent formation of Apaf-1/caspase-9 complex initiates an apoptotic protease cascade. Cell 91: 479–489
7. Liu XS, Zou H, Slaughter C and Wang XD (1997) DFF, a heterodimeric protein that functions downstream of caspase-3 to trigger DNA fragmentation during apoptosis. Cell 89: 175–184
8. Bossy-Wetzel E, Newmeyer DD and Green DR (1998) Mitochondrial cytochrome c release in apoptosis occurs upstream of DEVD-specific caspase activation and independently of mitochondrial transmembrane depolarization. EMBO J. 17: 37–49
9. Higuchi M, Proske RJ and Yeh ETH (1998) Inhibition of mitochondrial respiratory chain complex I by TNF results in cytochrome c release, membrane permeability transition, and apoptosis. Oncogene 17: 2515–2524
10. Martinou I, Desagher S, Eskes R, Antonsson B, Andre E, Fakan S and Martinou JC (1999) The release of cytochrome c from mitochondria during apoptosis of NGF-deprived sympathetic neurons is a reversible event. J Cell Biol. 144: 883–889
11. Single B, Leist M and Nicotera P (1998) Simultaneous release of adenylate kinase and cytochrome c in cell death. Cell Death Differ. 5: 1001–1003
12. Li F, Srinivasan A, Wang Y, Armstrong RC, Tomaselli KJ and Fritz LC (1997) Cell-specific induction of apoptosis by microinjection of cytochrome c – Bcl-x_L has activity independent of cytochrome c release. J. Biol. Chem. 272: 30299–30305
13. Zhivotovsky B, Orrenius S, Brustugun TO and Doskeland SO (1998) Injected cytochrome c induces apoptosis. Nature 391: 449–450
14. Garland JM and Rudin C (1998) Cytochrome c induces caspase-dependent apoptosis in intact hematopoietic cells and overrides apoptosis suppression mediated by Bcl-2, growth factor signaling, MAP-kinase-kinase, and malignant change. Blood 92: 1235–1246
15. Reed JC (1997) Cytochrome c – can't live with it – can't live without it. Cell 91: 559–562
16. Cai JY, Yang J and Jones DP (1998) Mitochondrial control of apoptosis – the role of cytochrome c. Biochim. Biophys. Acta 1366: 139–149
17. Chang S, Phelps P, Berezesky I, Ebersperger M and Trump B (2000) Studies on the mechanisms and kinetics of apoptosis induced by microinjection of cytochrome c in rat kidney tubule epithelial cells (NRK-52E). Am. J. Path. 156: 637–649
18. Salvioli S, Ardizzoni A, Franceschi C and Cossarizza A (1997) JC-1, but not $DIOC_6$(3) or rhodamine 123, is a reliable fluorescent probe to assess $\Delta\Psi_{mit}$ changes in intact cells – implications for studies on mitochondrial functionality during apoptosis. FEBS Lett. 411: 77–82

19. Metivier D, Dallaporta B, Zamzami N, Larochette N, Susin SA, Marzo I and Kroemer G (1998) Cytofluorometric detection of mitochondrial alterations in early CD95/Fas/Apo-1-triggered apoptosis of Jurkat T lymphoma cells – comparison of seven mitochondrion-specific flurochromes. Immunol. Lett. 61: 157 – 163
20. Okada CY and Rechsteiner M (1982) Introduction of macromolecules into cultured mammalian cells by osmotic lysis of pinocytic vesicles. Cell 29: 33 – 41
21. Thornberry NA, Ranon TA, Pieterson EP, Rasper DM, Timkey T, Garcialcalvo M, Houtzager VM, Nordstrom PA, Roy S, Vaillancourt JP, Chapman KT and Nicholson DW (1997) A combinatorial approach defines specificities of members of the caspase family and granzyme B – functional relationships established for key mediators of apoptosis. J. Biol. Chem. 272: 17907 – 17911
22. Waterhouse NJ, Finucane DN, Green DR, Elce JS, Kumar S, Alnemri ES, Litwack G, Khanna KK, Lavin MF and Watters DJ (1998) Calpain activation is upstream of caspases in radiation-induced apoptosis. Cell Death Differ. 5: 1051 – 1061
23. Duckett CS, Li F, Wang Y, Tomaselli KJ, Thompson CB and Armstrong RC (1998) Human IAP-like protein regulates programmed cell death downstream of Bcl-x_L and cytochrome c. Mol. Cell Biol. 18: 608 – 615
24. Brustugun OT, Fladmark KE, Doskeland SO, Orrenius S and Zhivotovsky B (1998) Apoptosis induced by microinjection of cytochrome c is caspase-dependent and is inhibited by Bcl-2. Cell Death Differ. 5: 660 – 668
25. Deshmukh M and Johnson EM (1998) Evidence of a novel event during neuronal death – development of competence-to-die in response to cytoplasmic cytochrome c. Neuron 21: 695 – 705
26. Neame SJ, Rubin LL and Philpott KL (1998) Blocking cytochrome c activity within intact neurons inhibits apoptosis. J. Cell Biol. 142: 1583 – 1593
27. Slee EA, Keogh SA and Martin SJ (2000) Cleavage of BID during cytotoxic drug and UV radiation-induced apoptosis occurs downstream of the point of Bcl-2 action and is catalysed by caspase-3: a potential feedback loop for amplification of apoptosis-associated mitochondrial cytochrome c release. Cell Death Differ. 7: 556 – 565
28. Nieminen AL, Petrie TG, Lemasters JJ and Selman WR (1996) Cyclosporin A delays mitochondrial depolarization induced by N-methyl-D-aspartate in cortical neurons – evidence of the mitochondrial permeability transition. Neurosci. 75: 993 – 997
29. Gilmore K and Wilson M (1999) The use of chloromethyl-X-rosamine (Mitotracker red) to measure loss of mitochondrial membrane potential in apoptosis cells is incompatible with cell fixation. Cytometry 36: 355 – 358
30. Scarlett JL and Murphy MP (1997) Release of apoptogenic proteins from the mitochondrial intermembrane space during the mitochondrial permeability transition. FEBS Lett 418: 282 – 286
31. Patterson SD, Spahr CS, Daugas E, Susin SA, Irinopoulou T, Koehler C and Kroemer G (2000) Mass spectrometric identification of proteins released from mitochondria undergoing permeability transition. Cell Death Differ. 7: 137 – 144
32. Chen Q, Gong B and Almasan A (2000) Distinct stages of cytochrome c release from mitochondria: evidence for a feedback amplification loop linking caspase activation to mitochondrial dysfunction in genotoxic stress induced apoptosis. Cell Death Differ. 7: 227 – 233
33. Li HL, Zhu H, Xu CJ and Yuan JY (1998) Cleavage of Bid by caspase 8 mediates the mitochondrial damage in the Fas pathway of apoptosis. Cell 94: 491 – 501
34. Bossy-Wetzel E and Green DR (1999) Caspases induce cytochrome c release from mitochondria by activating cytosolic factors. J. Biol. Chem. 274: 17484 – 17490
35. Marzo I, Susin SA, Petit PX, Ravagnan L, Brenner C, Larochette N, Zamzami N and Kroemer G (1998) Caspases disrupt mitochondrial membrane barrier function. FEBS Lett. 427: 198 – 202
36. Enari M, Talanian RV, Wong WW and Nagata S (1996) Sequential activation of ICE-like and CPP32-like proteases during Fas-mediated apoptosis. Nature 380: 723 – 726
37. Petit PX, O'Connor JE, Grunwald D and Brown SC (1990) Analysis of the membrane potential of rat- and mouse-liver mitochondria by flow cytometry and possible applications. Eur. J. Biochem. 194: 389 – 397
38. Nieminen AL, Byrne AM, Herman B and Lemasters JJ (1997) Mitochondrial permeability transition in hepatocytes induced by t-BuOOH: NAD(P)H and reactive oxygen species. Am. J. Physiol. - Cell Physiol. 41: C1286 – C1294
39. Petronilli V, Miotto G, Canton M, Brini M, Colonna R, Bernardi P and Di Lisa F (1999) Transient and long-lasting openings of the mitochondrial permeability transition pore can be monitored directly in intact cells by changes in mitochondrial calcein fluorescence. Biophys. J. 76: 725 – 734